CIRCUITS SYSTEMS SIGNAL PROCESS
VOL. 5, NO. 3, 1986

CHAOS GENERATION USING BINARY HYSTERESIS*

Robert W. Newcomb[1] *and Nevine El-Leithy*[1]

Abstract. The design of a continuous-time system suitable for electronic circuit realization for integrated circuit generation of chaotic responses is presented. The system is second order and is based upon an unstable oscillator with state-space trajectories that are fed back into themselves, and stabilized, via the use of binary hysteresis. The chaotic nature of the signals is guaranteed by a theorem of Li and Yorke through the generation of a period-three return map. Experimental results are given that verify the design.

1. Introduction

The mathematics of chaotic systems has recently been under great development and one can now cite hundreds of papers in the area (for which reason we will only cite those that are needed as we proceed). And, even though one can scarcely find engineering uses in the literature, it seems to us that there are some very meaningful ones. What has motivated us in this study, and indeed led to our collaboration, is fibrillation of the heart, which seems to us to be a chaotic mode. In our view very simple electronic systems which mimic such phenomena as fibrillation of the heart could lead to valuable noninvasive experimentation that could improve the quality of life for many individuals, for example by yielding control systems that bring a system out of chaos. Although we do not really say more about the heart in this paper, it may be well worth keeping it in mind to give motivation and orientation to the paper and to others in the field of chaotic circuits.

What we do is give the design theory and experimental results for a second-order, continuous-time, integrable electronic system which is shown

* Received May 22, 1985; revised February 14, 1986. Experimental results were supported by NSF Grant Numbers ENG ECS 83-17877 and ECS-85-06924.

[1] Microsystems Laboratory, Electrical Engineering Department, University of Maryland, College Park, MD 20742, USA

to give chaotic responses. We are able to achieve the chaotic responses in a second-order system by the use of binary hysteresis which is relatively easy to construct with transistorized circuits and which does seem relevant to the actual pumping of the heart. The philosophy, which is intuitively explained more fully in Section 2 before the mathematical and experimental developments which follow, is to create two planes in which second-order linear but unstable system "pseudo"-trajectories are formed. Via the hysteresis the true trajectories jump between these "pseudo"-trajectories in such a manner that the jump points are eventually fed inside themselves so that a period-three return map is generated. We then apply the mathematical result which shows that period three implies chaos [1]; we try to explain a little of the reasoning behind why period three implies chaos in the Appendix since we have found this to be a rather obscure point even to those well versed in the field. The system itself is presented in Section 3 while the mathematics for showing that chaos is indeed generated is developed in Section 4. Experimental results are presented in Section 5. The idea of using hysteresis stems from a comment of Rössler [2, p. 379] whose papers on the subject of chaos show considerable physical insight into the mechanisms involved. Here we extend and review some of the concepts outlined in our previous but not too available works [3], [4] while introducing experimental results which show the practical feasibility of the theory.

2. Binary hysteresis generation of period-three curves

In this section we outline the main ideas in an intuitive manner to try to give some physical insight into how we have proceeded to create the hysteretic degree-two oscillator. To understand the philosophy of operation of our system consider Figure 1 where we give a three-dimensional illustration representative of the process for the normalized case discussed below. In Figure 1 there are two parallel half-planes which overlap, the overlap being considered as accomplished through hysteresis. We think of each of the half-planes as half of the state space of a linear unstable degree-two oscillator. When a trajectory, which will be a spiral, of one of these oscillators reaches the edge of its half-plane it jumps to the other half-plane by virtue of the hysteresis, as illustrated by the indicated trajectory. Going through this we may trace a portion of the overall trajectory in Figure 1, by starting at point 1, which is also labeled a, in the lower plane and following the lower-plane curve through the lower plane, passing through points 2 and 3 (which is also point b) until it reaches the hysteresis jump line at point 4 where the trajectory jumps to the upper-plane spiral at point 5 and then follows that spiral until it again hits the edge of the hysteresis at point 6 where it next jumps down to point 7, etc., eventually passing through points c and d on the upper half x_2-axis. We control the nature of the overall trajectory then by the spiral parameters, the placement of the centers

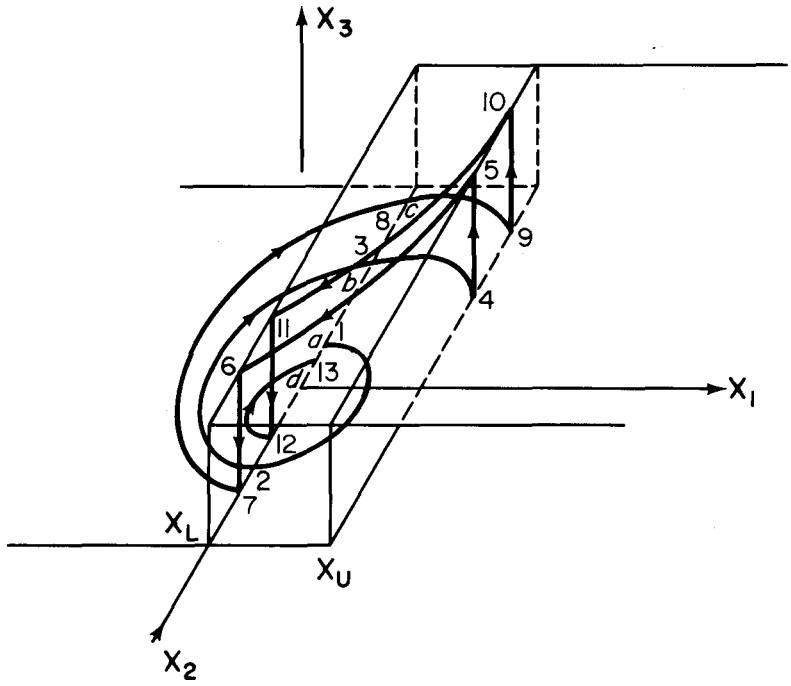

Figure 1. Three-dimensional view of system operation.

of the spirals being a critical factor. Indeed, we configure the spirals such that when some of the lower-plane spirals return to the lower plane, after traveling in the upper plane, they are closer to the center of the lower-plane spirals than before their jump to the upper plane. In Figure 1 this is indicated by point $1 = a$ coming back to point $13 = d$ on its return to the x_2-axis. Of importance is our monitoring of lower-plane spirals as they cross the upper half of the x_2 axis. If we plot the point of return to this half axis versus the point of previous crossing (of the upper half x_2-axis) we obtain an "upper half axis return map", which can be thought of as the input-output map $M(\cdot)$ of a discrete-time system as discussed more fully in Section 4. By adjusting our chaos oscillator system parameters we can make this return map continuous as well as having a point of period three, that is such that the thought of discrete-time system has a periodic trajectory which is periodic with least period three. More specifically point a of Figure 1 leads to point b and that in turn to point c and finally to point d which can be made equal to a to achieve period three. We then apply the theorem of Li and Yorke [1, p. 987] which shows that for an uncountable set of initial points (equivalent to crossing points of the positive x_2-axis in Figure 1) a discrete system with a period-three point has trajectories that are chaotic. The mathematical definition of chaos used by Li and Yorke for this discrete

system is that given two distinct starting points in this uncountable set then eventually the two resulting trajectories will move away from each other as well as come arbitrarily close. Since points on the trajectories of the discrete system are also points on the true continuous-time trajectories the latter will have the same chaotic properties, again as discussed more fully in Section 4.

To achieve the desired return map with a period-three point we can consider the two hysteresis half-planes mentioned above but now extended to full planes, each of which is the state space of a linear second-order unstable oscillator, as mentioned above. These two state-space planes can be projected one on the other and the trajectories of the separate oscillators (drawn in the full planes) superimposed, as shown in Figure 2, where the upper plane gives the upper left centered spiral and the lower plane the other (lower right centered) spiral. Then the actual trajectory of our chaos oscillator will consist of portions of the upper spiral to the right of x_L and portions of the lower spiral to the left of x_U, where x_L and x_U correspond to the hysteresis jump lines (for jumping to the upper and to the lower planes, respectively) as indicated in Figure 1 and labeled in Figure 2. The darkened path beginning at I illustrates the process.

To guarantee chaotic behavior we move one of the spiral centers (in our case the upper one) around until a spiral in one plane, in Figure 2 the spiral R of the lower plane, becomes fed back closer to its origin after a cycle of jumps through the hysteresis. Then we choose the system parameters such that the upper axis return map is continuous in order to apply the theorem of Li and Yorke; Figure 3 shows the return map $M(\cdot)$ that results from the set of parameters developed in the following sections. At first glance it appears that this will require two independent degree-two oscillators, but, remarkably, as we will see, the process can be accomplished by one second-order oscillator with a parameter shift of the state-space origin controlled by the hysteresis, in which case the overall oscillator need be only a degree-two system.

3. The hysteretic chaotic system

In this section we develop the system equations for our design. An example realization in terms of electronic circuits is given in Section 5.

We begin with semistate type equations in a form suitable for our electronic realization, this being

$$dX_1/dt = \omega_0 X_2 + a_1 \omega_0 H(X_3), \tag{1a}$$

$$dX_2/dt = -\omega_0 X_1 - 2\sigma\omega_0 X_2 + a_2 \omega_0 H(X_3), \tag{1b}$$

$$X_3 = b_1 X_1 + b_2 X_2, \tag{1c}$$

for which a signal flow graph is shown in Figure 4 (where $1/\omega_0 s$ denotes

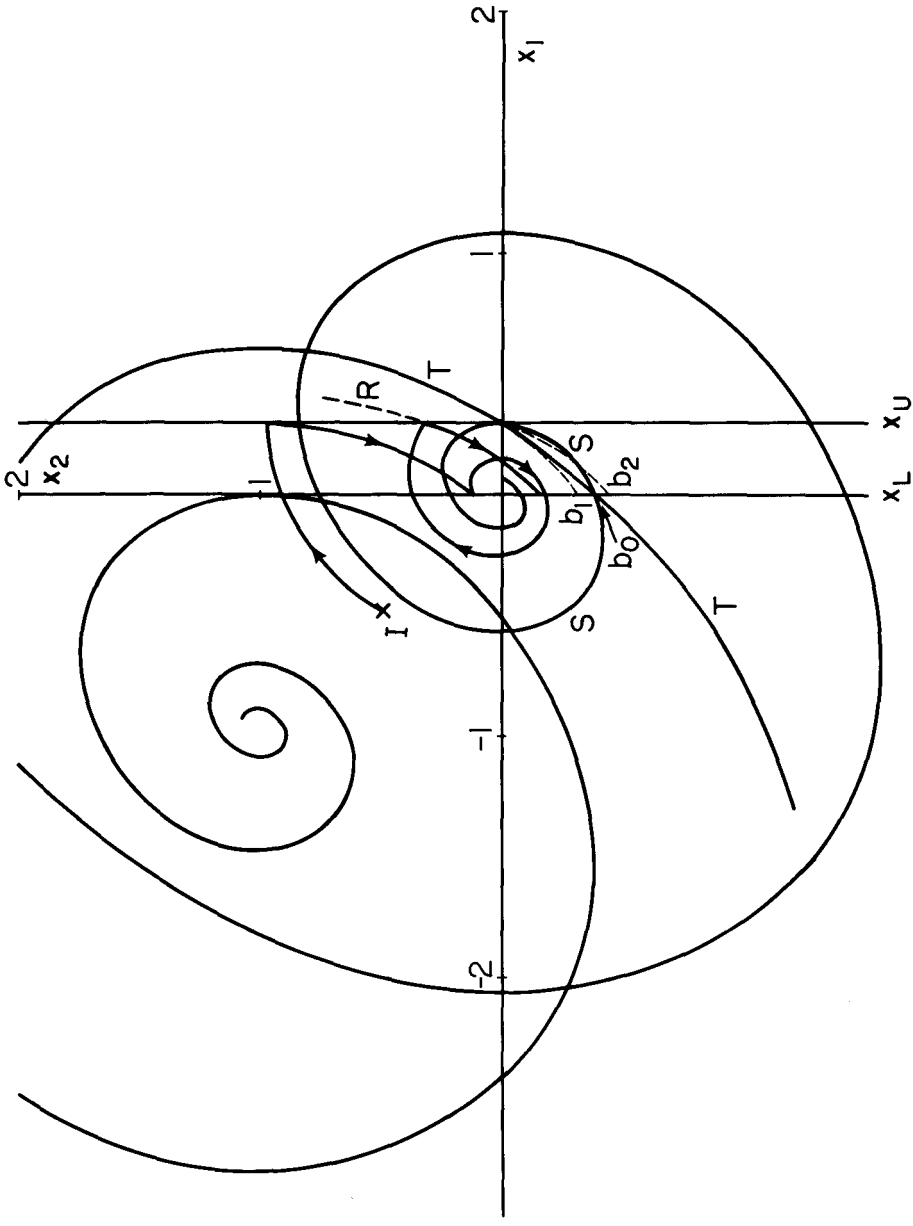

Figure 2. Spiral overlay.

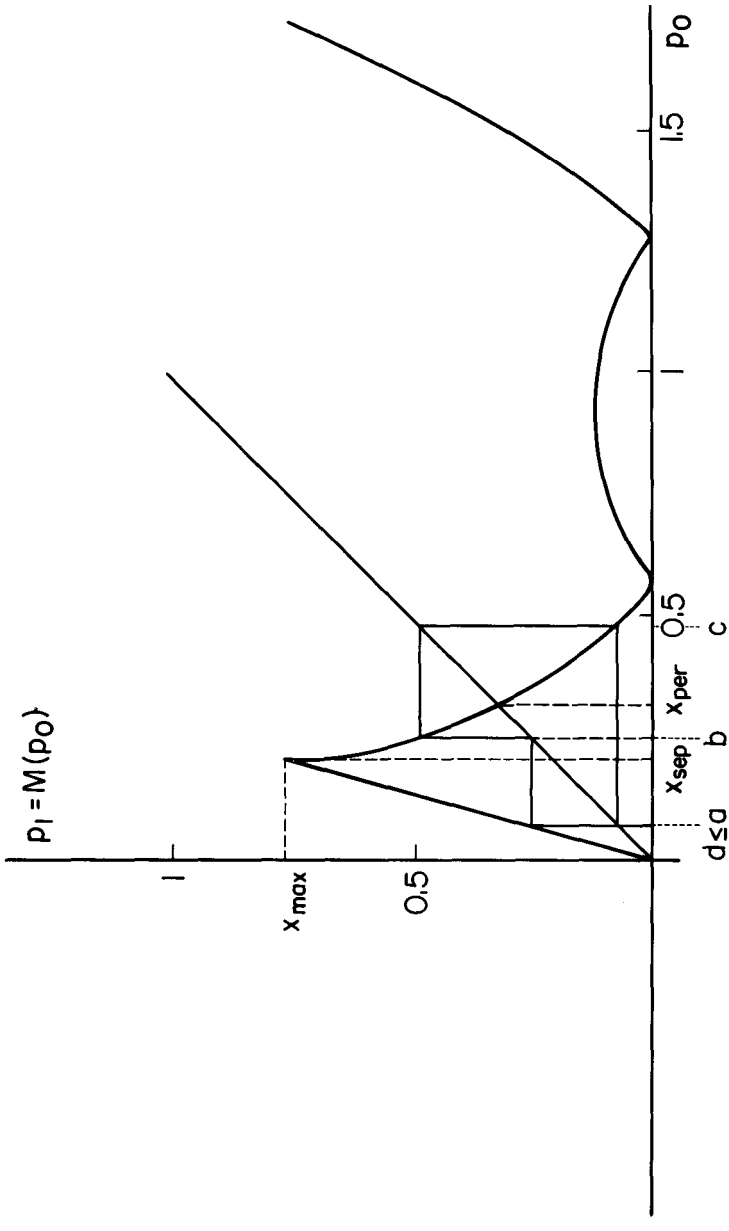

Figure 3. Upper half axis return map for $\sigma = -0.2$, $x_L = 0$, $x_U = -0.3$, $a_2 = -1.3499+$ having $x_{sep} = 0.20893+$, $x_{max} = 0.75339+$ and $a = d = 0.06925+$, $b = 0.24971+$, $c = 0.06925+$.

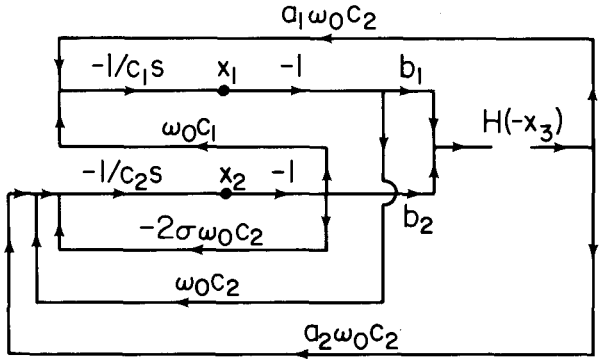

Figure 4. Signal-flow graph.

an integrator of time scale ω_0). Here $H(\cdot)$ is a binary hysteresis taking the values

$$H(X_3)=\begin{cases} H_+ & \text{for } X_L < X_3 \text{ (upper branch)}, \\ H_- & \text{for } X_3 < X_U \text{ (lower branch)}, \end{cases} \tag{2}$$

and the system design parameters a_1, a_2, b_1, b_2, σ, and ω_0 are constants to be specified by our designs. We, therefore, have two cases depending upon on which of the two hysteresis branches the system resides at a given instant and in each case the system acts as a degree-two unstable system since we now specify a negative damping factor, $\sigma < 0$. The equilibrium points of the two subsystems are

$$(X_1, X_2)_U = ([2\sigma a_1 + a_2]H_+, -a_1 H_+), \tag{3a}$$

$$(X_1, X_2)_L = ([2\sigma a_1 + a_2]H_-, -a_1 H_-), \tag{3b}$$

from which we see that we have freedom to move these equilibrium points independently via system design parameters. For simplicity we choose the hysteresis dependence to be only upon X_1, that is we specify as a design criteria

$$b_1 = 1, \qquad b_2 = 0. \tag{4}$$

The key to a clear understanding of our system is a set of normalizing transformations [3] which puts into evidence the control of the design parameters on the system characteristics. First we transform the lower hysteresis value to zero and then move the lower equilibrium point to the origin via

$$\mathbf{X}_2 = X_2 + a_1 H_-, \tag{5a}$$

$$\mathbf{X}_1 = X_1 - [2\sigma a_1 + a_2]H_-, \tag{5b}$$

while, in order to work with a normalized hysteresis amplitude of unity,

we scale by the hysteresis height

$$x_1 = \mathbf{X}_1/[H_+ - H_-], \tag{5c}$$

$$x_2 = \mathbf{X}_2/[H_+ - H_-]. \tag{5d}$$

These normalizations also scale the hysteresis jump lines, X_L and X_U, which in normalized form we now call x_L and x_U.

At this point have a normalized set of equations

$$x_1' = x_2 + a_1 h(x_1), \tag{6a}$$

$$x_2' = -x_1 - 2\sigma x_2 + a_2 h(x_1), \tag{6b}$$

where $'$ denotes differentiation with respect to normalized time, $' = d/d(\omega_0 t)$, and where the hysteresis is of the form

$$h(x) = \begin{cases} 1 & \text{for } x_L < x, \\ 0 & \text{for } x < x_U. \end{cases} \tag{6c}$$

As seen from (3), in the (x_1, x_2)-plane the equilibrium points of the two subsystems are at the origin for the lower-plane case, and at

$$(x_1, x_2)_U = (2\sigma a_1 + a_2, -a_1) \tag{6d}$$

for the upper-plane sprials. We thus see that the ratio of σa_1 to a_2 is the design parameter for fixing the relative locations of the two spirals. For convenience we choose

$$a_1 = -1, \tag{6e}$$

which could be considered as a further scaling of the hysteresis which turns it over while placing the upper-plane spiral's center on the line $x_2 = 1$. By one more change of variables we can bring our equations in both the upper and the lower planes to the form

$$x' = y, \tag{7a}$$

$$y' = -x - 2\sigma y, \tag{7b}$$

where our final transformations are

	lower plane		upper plane	
$x =$	x_1	or	$x_1 - 2\sigma a_1 - a_2$,	(7c)
$y =$	x_2	or	$x_2 + a_1$.	(7d)

From (7a, b) we see that the design parameter, σ, controls the shape of the spirals and that the spirals in the upper plane are identical to the ones in the lower plane except for the shift in their origin (this shift being given by (6d) which is rephrased in (7c, d), both subject now to $a_1 = -1$). For design purposes we can then construct a set of universal solutions to (7),

these being spirals [5, p. 127], one spiral for each σ (the calculations being given below in (9)), and then working with a pair of identical spirals overlayed one on top of the other. By shifting the origin of the top sprial along the $x_2 = 1$ line the various characteristics can be changed and with some experience one gets a good feeling for the nature of the resulting system. Figure 2 gives a typical view of one set of spirals overlaid on the other. Finally we have x_U and x_L as parameters still to be chosen. Because it allows analytic treatment for some of the behavior, we conveniently choose

$$x_L = 0. \tag{8a}$$

In the end then we are left with a_2, x_U, and σ as parameters free to be chosen (with x_U positive and the other two negative). To make things concrete we give our choices for much of the following discussion as

$$x_U = 0.3, \tag{8b}$$

$$\sigma = -0.2, \tag{8c}$$

$$a_2 = -1.34996673232527. \tag{8d}$$

Here σ is picked as a convenient number with a_2 chosen to ensure continuity of the upper half-axis return map.

The numerical results used for Figures 2 and 3 were obtained by explicitly solving (7) by putting the solutions in the form

$$x(t) = K(\exp[-\sigma t])\cos[\omega t + \varphi], \tag{9a}$$

$$y(t) = K(\exp[-\sigma t])\cos[\omega t + \varphi + \measuredangle s], \tag{9b}$$

where

$$\omega = (1-\sigma^2)^{1/2}, \tag{9c}$$

$$\measuredangle s = \arctan[\omega/(-\sigma)] = \text{angle of } -\sigma + j\omega, \tag{9d}$$

and the "radius" constant, K, and angle, φ, of the spiral are determined from initial conditions

$$x(0) = X \quad \text{and} \quad y(0) = Y \tag{9e}$$

according to whether $x(0)$ is nonzero or not by

$$\begin{aligned} &\text{if } X \neq 0 && \text{if } X = 0 \\ &K = [\operatorname{sign} X][X^2 + 2\sigma XY + Y^2]^{1/2}/\omega \quad \text{or} \quad K = -Y/\omega, && (9f) \\ &\varphi = \arcsin[(Y + \sigma X)/(-\omega K)] \quad \text{or} \quad \varphi = \pi/2 && (9g) \\ &\quad = \arctan[(Y + \sigma X)/(-\omega X)]. \end{aligned}$$

Equations (7c, d) are used to evaluate the initial conditions X, Y to be used in (9). Of particular interest to this is the starting point. We see that if $X_1(0) = X_2(0) = 0$ then we are in the lower hysteresis plane and (from (5) and 7(c, d)) $x(0) = a_1 H_-/[H_+ - H_-]$, $y(0) = (2\sigma a_1 + a_2)H_-/[H_+ - H_-]$ which actually give the initial point I in Figure 3.

4. Chaotic nature of the system

With the system as described above now on hand we can proceed to develop some of the fascinating properties it possesses. Since our notion and proof of chaotic behavior rests upon the theorem of Li-Yorke, we first give a statement of that theorem. Following that in Section 4.2 we show how we satisfy the theorem's conditions and then in Section 4.3 we show the consequences for our continuous-time system.

4.1. The Li-Yorke theorem [1, p. 987]

This theorem considers iterates of continuous maps M where we denote the nth iterate of M by M^n and which means M^{n-1} acting on M for nonnegative integers n; we take $x = M^0(x)$ and have $M^n(x) = M^{n-1}(M(x))$ for x in the domain of definition of M. By a periodic point of period k for M is meant a point p in the domain of M for which $p = M^k(p)$ but $p \neq M^n(p)$ for $n < k$, for k and n positive integers. The Li-Yorke theorem is then as follows:

Let M be a continuous map of an interval J into itself such that there is a point a in J for which the first iterate $b = M(a)$, the second iterate $c = M(b)$, and third iterate $d = M(c)$ satisfy

$$d \leq a < b < c. \tag{10a}$$

Then the following properties, (1), (2), and (3), hold:

(1) There is an uncountable set S contained in J and containing no periodic points for whch the following holds: for every p and q in S with $p \neq q$

$$\limsup_{n\to\infty} |M^n(p) - M^n(q)| > 0, \tag{10b}$$

$$\liminf_{n\to\infty} |M^n(p) - M^n(q)| = 0. \tag{10c}$$

(2) For every k there is a periodic point in J of period k.

(3) For every p in S and every periodic point q in J

$$\limsup_{n\to\infty} |M^n(p) - M^n(q)| > 0. \tag{10d}$$

It is convenient to call the points in S chaotic points in which case property (1) is seen to be the chaos property in that it states that any two chaotic points eventually keep wandering away from each other while also coming arbitrarily close interminably. The third property essentially states that the chaotic points cannot turn into periodic ones; but looked at another way (as seen in Li-Yorke's proof) it really means that periodic points near chaotic ones are unstable and can turn into chaotic points under small perturbations. We comment that M can be considered as a discrete-time

map, $x^{k+1} = M(x^k)$, of discrete time k and that property (1) holds when M has $d = a$, that is when a period-three point exists.

4.2. *Satisfaction of the Li-Yorke theorem*

The map to which we wish to apply the Li-Yorke theorem is the upper half axis return map with a representation shown in Figure 3 (where a unity slope line is superimposed for ease of later discussions). Concerning this map we first make the following observations. When, for this map, we restrict its argument to be between 0 and 1 (or even 1.5) we see on viewing Figure 3 that the largest value taken by this map is around $\frac{3}{4}$. Thus, we can consider the interval J to be the interval [0, 1], since this interval is mapped into itself. This map will be shown to be continuous and to have a period-three point. Hence, the conditions of the Li-Yorke theorem will be satisfied by this map and there is a chaotic subset S of the interval [0, 1].

4.2.1. Construction of the upper half axis return map. To construct the upper half axis return map we pick a point p_0 on the upper x_2-axis as illustrated in Figure 5. The trajectory staring at this point at time t_0 eventually returns to the upper half x_2-axis at point p_1 and time t_1, as shown in Figure 5 where t_1 is the next time at which such a return occurs. By definition p_1 is the first upper half axis return point of p_0; the map M that yields p_1 from p_0 for any nonnegative p_0 is the upper half axis return map. If we place ourselves on

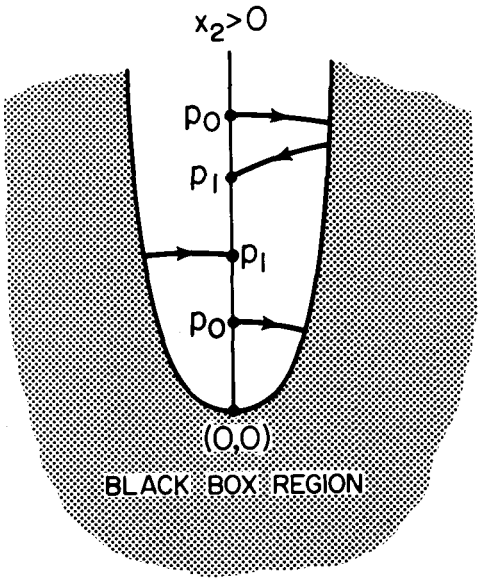

Figure 5. Upper half axis returns.

the upper x_2-half-axis at any point p_0 and surround this half axis by a "black box," as shown in Figure 5, we can construct this map by simply noting the point p_1 where the trajectory next hits this half axis, irrespective of where it has gone in the black box between p_0 and p_1. Of course, to make a calculation on the computer to find p_1 given p_0 we need to keep track of where the trajectory goes. This is actually a bit messy since there are several possibilities. These possibilities can be broken into two cases, that for which the trajectory remains completely in the lower hysteresis plane and that for which a switch is made into the upper hysteresis plane. Treating first the possibility in which the trajectory remains on a lower-plane spiral throughout the path in going from p_0 to p_1, since a rotation of 360° is made, from (9a, f) we obtain

$$p_1 = p_0 \exp(-2\sigma\pi/\omega). \tag{11a}$$

This holds for p_0 smaller than the value for which the maximum value of x_1 on one turn of the spiral starting at p_0 is x_U; we call x_{sep} the value of this p_0 since it separates spirals into two classes, those which stay completely in the lower hysteresis plane during a revolution (for $p_0 < x_{sep}$) and those that jump to the upper hysteresis plane. By setting x_2, which is the derivative of x_1 in the lower hysteresis plane, equal to zero, we find the maximum of x_1 using (9b). Setting this maximum equal to x_U leads to

$$x_{sep} = x_U \exp((\sigma/\omega)(\pi + \arctan(\omega/\sigma))). \tag{11b}$$

The maximum value of p_1 obtained in the range of interest (for p_0 in [0, 1] for Figure 3) is then

$$p_1 = x_{max} = x_{sep} \exp(-2\sigma\pi/\omega). \tag{11c}$$

In the remaining case the trajectories switch between the lower and upper (at $x_1 = x_U$) and then back to the lower (at $x_1 = 0$) hysteresis planes. In doing this there are several possibilities. Among these possibilities are again two cases, one case being that the trajectory returns to $x_1 = 0$ with x_2 nonnegative, in which case the x_2 value is p_1; in the other case the return to $x_1 = 0$ is with $p_1^* = x_2 < 0$ in whch case a 180° rotation is still required to bring $x_2 > 0$ (thus, $p_1 = -p_1^* \exp(-\sigma\pi/\omega)$). In either of these latter two subcases there are again two possibilities, one being that the upper-plane spirals are hit before they obtain their x_1 maximum, in which case they spiral back through $x_1 = x_U$ before returning to the lower plane at $x_1 = 0$ (this accounts for the region after the local peak near $p_0 = 1$ in Figure 3). Finally, there is the subcase where the upper-plane spiral is hit with its x_2 value below 1 when the lower-plane spiral achieves $x_1 = x_U$. For calculation of all of these subcases of returns we have, as yet, no such analytic formulas as in (11) but the calculations are straightforward using (9), and curves of the nature of Figure 3 will result for values of the design parameters near those given.

It should be noted that a map of the next return to the lower half x_2-axis looks very similar to the negative of that for the upper half x_2-axis; this is as expected since, if we find chaos in the peak of a waveform of the kind under discussion, we also expect chaos in the minima, and the minima are related to the returns to the lower half-axis. It should also be mentioned that the half x_2-axis return maps are related to the returns at any point of the x_2-axis via a composition process. This composition is rather messy since in some cases there are two returns to the full axis before one to the half-axis, while in other cases there is just one return. Thus, one must be careful not to throw away any returns in obtaining the half-axis results from the full axis returns. In any event we are really after the upper half-axis return map since it is that which relates directly to the peak of the real time $x_2(t)$ signal upon which the chaos is readily seen experimentally.

4.2.2. Continuity of the map. In fact the upper half-plane map is generally not continuous since there is a break at $p_0 = x_{\text{sep}}$. However, there is a choice of the design parameter a_2 which guarantees continuity, as we show here. Considering Figure 2 we see that the condition for continuity of the upper half axis return map is that the upper hysteresis plane spiral, T on the figure, passing through $x_1 = x_U$ and $x_2 = 0$ also passes at $x_1 = 0$ through the same x_2 point, b_0 on the figure, as the separating spiral S. By making a_2 less negative we make the upper-plane spiral cut more sharply across $x_1 = x_L$, and thus, if it originally cuts at b_2 in Figure 2, we can move it to b_1 and vice versa, by making a_2 more negative. For example, when $\sigma = -0.2$ for $a_2 = -1.3$ we find $b_2 = -0.407978164$ while for $a_2 = -1.4$ we find $b_1 = -0.385451946$. Thus, by continuity of the solutions of ordinary differential equations in the parameters [6, p. 101], we can find a value b_0 such that the two spirals S and T "intersect" at $x_1 = x_L$. As it turns out the spiral T can be represented analytically in terms of the design parameters, and, hence, an (implicit) equation obtained which yields a_2 to guarantee the desired continuity. Specifically, (9a, b) yield [6, p. 20]

$$x^2 + ((\sigma x + y)/\omega)^2 = K^2 \exp((2\sigma/\omega)[\pi + \varphi + \arctan((\sigma x + y)/(\omega x))]), \tag{12a}$$

which is evaluated on the upper hysteresis plane using (7c, d) and $x_1 = 0$ with $x_2 = b_0$, where b_0 is found using a 180° rotation on $p_0 = x_{\text{sep}}$ from (11b). We calculate

$$b_0 = -x_{\text{sep}} \exp(-\sigma\pi/\omega). \tag{12b}$$

For $\sigma = -0.2$ we find, from (12a, b), $a_2 = -1.34996673232527+$ as the a_2 value to give continuity and for $\sigma = -0.191298828125+$, which is a value of particular interest as discussed below, $a_2 = -1.33449329331925+$.

4.2.3. Period-three points. The fact that the upper half axis return map, Figure 3, is teepee-like with magnitude of slopes greater than unity between

the first two zeros guarantees period-three points on either side of the peak between the zeros. These are shown on the figure for which the unity slope line has been superimposed to aid visualization. Numerically one of these period-three points can be calculated by solving the system equations for a trajectory that starts on the upper half-axis and returns to it three times. Doing this, one finds for $\sigma = -0.2$ and $a_2 = -1.3499667323527$ that $a = 0.069253575003$ yields to within 10 digits $d = a$ and $b = 0.2497160815$, $c = 0.4916892030$ for period-three points. Perhaps more significantly for this same σ and a_2 one has for $a = 0.067$ that $b = 0.2415900906$, $c = 0.5182976251$, and $d = 0.03847065827 < a$. Since in this latter case $a - d > 0.02$ with calculations carried out to 16 places there should be no question of the validity of the result $d < a < b < c$ for this upper half axis return map even though the result is only verified numerically. It is of course significant that the absolute value of the slope of the upper half-axis return map is greater than unity since this guarantees that even if d were slightly greater than a, say as a result of numerical error, then a slight lowering of a will lower d even more and make it less than a.

In the case discussed below of $\sigma = -0.191298828125$ with $a_2 = -1.33449329331925$ (which are for a continuous return map with continuous-time peaks on the spiral maximum line) we find the period-three points $a = d = 0.0696783616394$, $b = 0.2495983577442$, and $c = 0.4910452522263$. The upper half-axis return map for this case is only imperceptively changed from that of Figure 3.

4.3. Continuous-time chaos

The fact that the discrete-time upper half-axis return map M exhibits chaos means that $x_2(t_0)$ is chaotic for those values of time t_0 for which $x_1(t_0) = 0$ and $x_2(t_0)$ is nonnegative. This implies that the (local) peak value of $x_2(t)$ is chaotic since the peak value of $x_2(t)$ is a monotonically nondecreasing continuous function of the value of x_2 at the upper half-axis crossing (with the function going through zero at zero). This monotonicity follows from the increasing distance between spirals as they unwind, as seen from figures such as Figure 2 and the continuity follows from the continuity of a spiral as a geometric curve and the continuity of spirals in their starting values. Then the lim inf and lim sup properties of (10) hold for peak values of the continuous-time x_2 trajectories. That is, if the lim sup is nonzero for upper axis x_2 values when $x_1 = 0$ then the lim sup will remain nonzero (in fact it will be larger) for peak x_2 values. Clearly, also, by the continuity, the peak values can be made arbitrarily close by choosing the upper half axis x_2 values arbitrarily close, in which case the lim inf property is transferred to the peak values. If the peak value occurs on the lower hysteresis plane portion of the trajectory, then an analytic relationship can be readily established for the peak x_2 value, call it $x_{2\,\mathrm{peak}}$, as a function of the

upper half x_2-axis crossing value p_0 (since the derivative of x_2 set equal to zero gives, by (7b), $x_1 = -\sigma x_2$ for the peak values, and this can be solved for the time $t_{\max}$ at which $x_{2\,\text{peak}}$ occurs); specifically, we find

$$t_{\max} = (1/\omega) \arctan[-2\sigma\omega/(1-2\sigma^2)], \tag{13a}$$

$$\sin(\omega t_{\max}) = -2\sigma\omega/(1-2\sigma^4), \tag{13b}$$

$$x_{2\,\text{peak}}(p_0) = (p_0/(1-2\sigma^4)) \exp((-\sigma/\omega) \arctan[-2\sigma\omega/(1-2\sigma^2)]). \tag{13c}$$

If this value of $x_{2\,\text{peak}}$ for $p_0 = x_{\max}$ (see Figure 3) is less than the intersection of the $x_1 = -2\sigma x_2$ line with $x_1 = x_U$ then $x_{2\,\text{peak}}(p_0)$ will always be linear in p_0. Such occurs for all $-\sigma \geq 0.191298828125$ as is found by solving

$$-x_U/(2\sigma) \geq x_{2\,\text{peak}}(x_{\max}) \tag{13d}$$

for σ, which, when written out using (13c), is

$$1 \geq (-2\sigma/(1-2\omega^4)) \exp((\sigma/\omega)[-\pi + \arctan(\omega/\sigma) - \arctan(-2\sigma\omega/(1-2\sigma^2))]). \tag{13e}$$

5. Experimental results

The theory was checked in two different ways, one by experimental measurements on an RC-op-amp circuit and the other via computer simulations on an IBM PC with initial calculations on an HP15C. The results are in almost perfect agreement with the theory, this being somewhat expected since in both cases we have reliable means to proceed; for the computer we have exact solutions to (7) and for the experiments we have good binary hysteresis available. Since the computer results are almost identical to the experimental ones we concentrate upon the latter here.

Figure 6 shows the circuit that was built, for which the following values were chosen for the system design parameters:

$\sigma = -0.2$,
$a_1 = -1$,
$a_2 = a_0 \approx -1.35$,
$H_+ = -H_- = 4$,
$x_L = 0$ which is $X_L \approx 3.8$, and
$x_U = 0.3$ which is $X_U \approx 6.2$.

In Figure 6 the capacitors C fix the time scale while the MOS circuitry associated with C fixes the initial conditions (which for the curves of Figure 7 were chosen as zero). The center of the lower spiral is at $x_1 = x_2 = 0$ which becomes, following the transformations of (5), $X_1 = (2\sigma a_1 + a_2)H_- \approx +3.8$, $X_2 = -a_1 H_- = -4$. Figure 7a) shows the trajectory in the X_1, X_2-plane. In Figure 7(a) one can see the center of the bottom spiral located as just mentioned and the switching of the trajectory as it hits the hysteresis edges

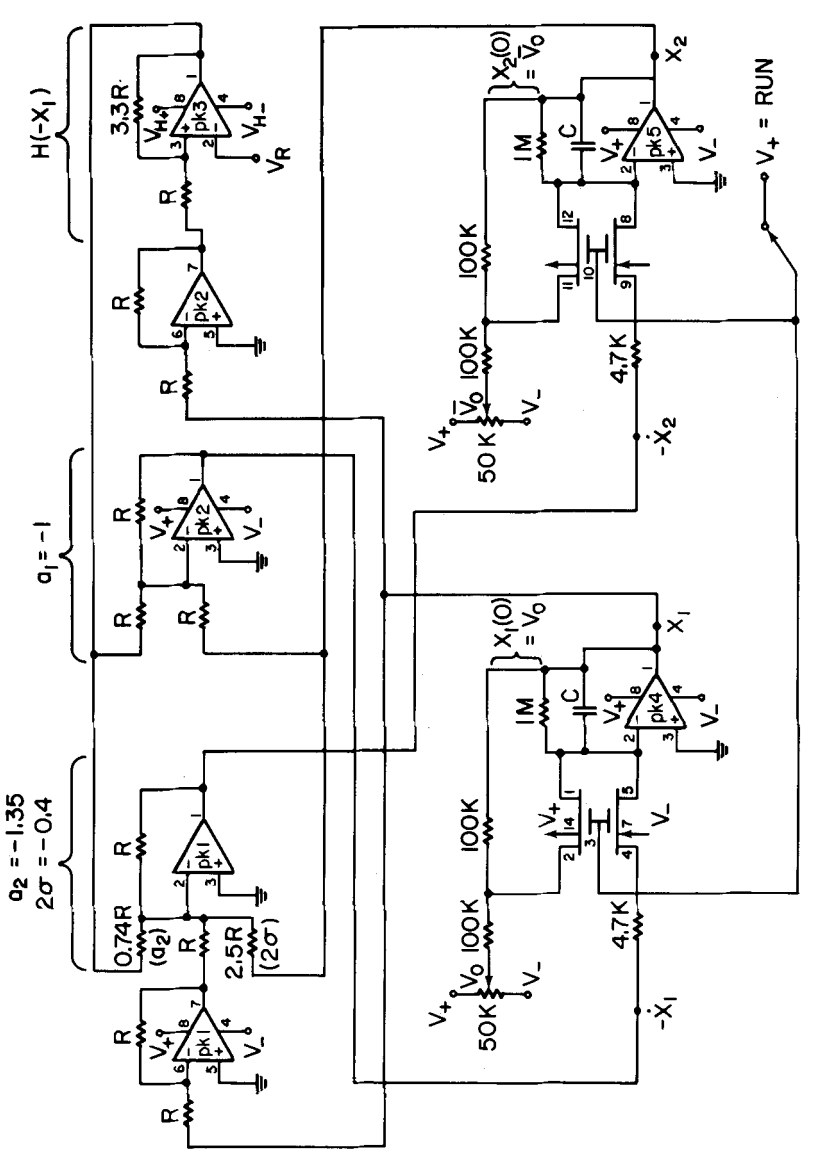

Figure 6. RC-op-amp circuit realization.

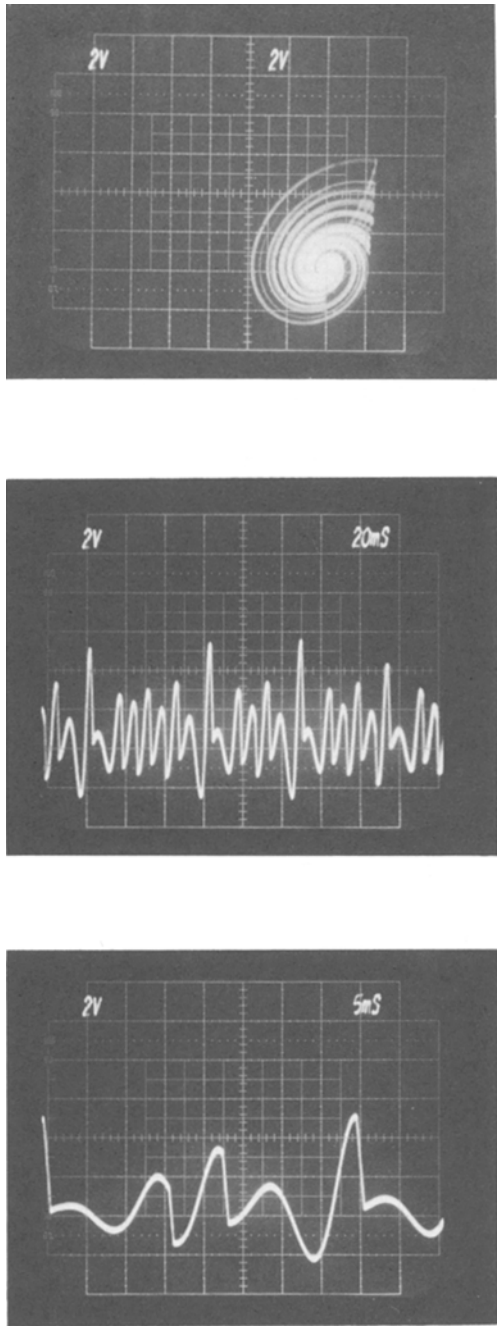

Figure 7. Chaos oscillator circuit responses: (a) phase plane trajectories; (0, 0) at midpoint; (b) $x_2(t)$; 0 at center graticule; (c) expanded view of $x_2(t)$. Op-amps = MC1458; CMOS switches = CD4007; $R = 100\ \text{k}\Omega$, $C = 0.32\ \mu\text{fd}$, $V_+ = -V_- = 10$ V, $V_R = -3.4$ V, $V_{H_+} = 4.2$ V, $V_{H_-} = -6.4$ V (to give $H_+ = -H_- = 4$ V).

at X_L and X_U. As can be seen also in that figure, the trajectory fills up a region of the plane, which is one criteria that can be used to indicate experimentally the possible presence of chaotic behavior. In Figure 7(b) a portion of the X_2 versus time response is shown with Figure 7(c) showing another portion on an expanded scale such that the switching action is seen in more detail.

6. Discussion

We have outlined here the theory and given experimental results on a degree-two chaos generator, with the framework set up for the design of such oscillators to be realized in integrated circuit form. Indeed, this system is ideal for such realization since it can be constructed directly, without inductors or other difficult-to-realize elements; nevertheless, one would still like to find even simpler structures for the future. It is of interest to note that at least degree three is required for a continuous-time chaos generator if continuous nonlinearities are used [7], in which case it is seen that the hysteresis is critical to obtaining the low degree. The philosophy of operation of our degree-two oscillator is such that one suspects that using hysteresis one might also be able to make a degree-one chaos oscillator. We note that previously we have been able to make a different type of chaos using bent hysteresis in a degree-three system [8].

We have set up the theory by using a set of transformations to obtain equations which isolate the important parameters and their functions. As such, the results here should be of further use in obtaining designs with specific properties. For example, by movement of the upper hysteresis jump line the upper amplitude of the x_1 response is completely controllable. Investigations into results of different ranges of parameters seems worth making especially if the system is to be applied in some useful situations. For this kind of study it would be appropriate to set up computer graphics so that one could see, on a display, the overlay of the two spiral systems and the effects on their intersections of parameter changes. What we have done on the computer is to set up the system solutions with print-outs that mimic the responses given in Figure 7(b) and (c) In making calculations of the total system response, we point out that the determination of the switching points is rather touchy, this being performed by determining the time for which a trajectory crosses a hysteresis jump line, $x_2 = x_L$ or x_U as the case may be, and then evaluating x_1 at this time.

We have based the development upon a continuous return map since the mathematical theorem used from the literature is stated for continuous maps. But continuity near the local peak in Figure 3 does not really appear necessary as a run through of the proof of Li and Yorke seems to indicate and experimentation on the circuit of Figure 6 bears out. Certainly in analog realizations trying to hold a_2 to the exact value needed to achieve continuity

of the upper half axis return map is not possible and this impossibility coupled with the results of Figure 6 indicates the robustness of the system.

Alternatively, as one reveiwer has very kindly pointed out, the fact that our upper half axis return map has a slope of absolute value greater than unity near the period-three points guarantees that there exists an absolutely continuous invariant measure in the region near the period-three points [9]. Such a result means that the signals behave in a probabilistic kind of manner [10, 11]. Although the definition for chaos in the presence of absolutely invariant measures is somewhat different than used here, and would most likely follow the notions of Wiener in introducing a concept of chaos [12], it seems just as meaningful physically, if not more so. As shown in [13] it is possible to have windows, essentially containing impulses, within an invariant measure (that would not be absolutely continuous) which allow for periodic continuous-time responses, even when there are period-three points; but that does not occur near the chaotic responses treated here. The reviewers have also called our attention to the degree-three RLC circuit of [14], reference to which has allowed us to obtain a closed form for the linear part of the half axis return map, and to [15], which would be useful in simulating the heart as a connection of oscillators (rather than the more primitive, but often more convenient, form of a single relaxation oscillator which we have had in mind [16]). In searching the literature that was helpfully called to our attention by the reviewers we also found [17] which uses a very similar half axis return map though found for a different system in a different situation.

Appendix

Period three and chaos

The result of Li and Yorke as quoted above is that if a map continuously transforms an interval into itself and has a period-three point then it has periodic points of all positive integer periods as well as a chaotic set. In the latter any two points are such that after a large enough number of iterations they sometimes become arbitrarily close while they also sometimes become sufficiently separated; as the number of iterations increases the number of iterations between, assuming the same values, changes somewhat randomly (this latter is developed in the proof of Li and Yorke but not really spelled out in their theorem, though in essence it is the basic principle of their type of chaos, it seems to us). The physical reasoning behind this is not elaborated in the literature as yet. What is clear is that the period-three points, a, b, and c of Figure 3, break the map into acting on two regions (one between a and b and one between b and c) with the peak point of the map in one of the regions. This has the effect that points in one of the regions are eventually mapped back into the other region. For a subset of

the two regions points never quite go back to the same place and, hence, iteration of them yields chaotic kinds of responses. For this phenomena to occur it does not appear necessary that the map be continuous at the local peak in the chaotic region (at x_{sep} in Figure 3), thus allowing for important extensions of the theorem of Li and Yorke. We note that if there is not a point of period three but one, say, of period five, the division of the region into two portions that are always mapped into each other does not occur and, hence, at first glance it seems that it may not be possible to generate a chaotic response. However, a theorem of Sharkovski shows that there are a number of divisions which could lead to chaos, including that coming from period five [18].

Acknowledgments

The authors wish to express their appreciation to the reviewers for their very helpful constructive comments, to Professor Zemanian for his interest, encouragement, and assistance in perfecting the presentation, and to N. Kusuma for drawing the figures to illustrate the concepts.

References

[1] T.-Y. Li and J. A. Yorke, Period three implies chaos, *Amer. Math. Monthly*, **82**, 985-992, 1975.

[2] O. E. Rössler, Continuous chaos—four prototype equations, in *Bifurcation Theory and Applications in Scientific Disciplines* (O. Gurel and O. E. Rössler, eds), pp. 376-392, Annals of the New York Academy of Sciences, Vol. 316, 1979.

[3] R. W. Newcomb and N. El-Leithy, A binary hysteresis chaos generator, *Proceedings of the* 1984 *IEEE International Symposium on Circuits and Systems*, Montreal, pp. 856-859, 1984.

[4] R. W. Newcomb and N. El-Leithy, Trajectory calculations and chaos existence in a binary hysteresis chaos generator, *Proceedings of the Fifth International Symposium on Network Theory*, Sarajevo, 1984.

[5] V. I. Arnold, *Ordinary Differential Equations*, MIT Press, Cambridge, MA, 1973.

[6] A. A. Andronov, A. A. Vitt, and S. E. Khaikin, *Theory of Oscillators* (translated by F. Immirzi and edited by W. Fishwick), Pergamon Press, Oxford, 1966.

[7] G.-Q. Zhong and F. Ayrom, Periodicity and chaos in Chua's circuit, *IEEE Trans. Circuits and Systems*, **32**, 501-503, 1985.

[8] R. W. Newcomb and S. Sathyan, An RC-op-amp chaos generator, *IEEE Trans. Circuits and Systems*, **30**, 54-56, 1983.

[9] T.-Y. Li and J. A. Yorke, Ergodic transformations from an interval into itself, *Trans. Amer. Math. Soc.*, **235**, 183-192, 1978.

[10] G. Pianigiani, On the existence of invariant measures, in *Applied Nonlinear Analysis* (V. Lakshmikantham, ed.), pp. 299-307, Academic Press, NY, 1979.

[11] A. Lasota, A solution of Ulam's conjecture on the existence of invariant measures and its applications, in *Dynamical Systems*, Vol. 2 (L. Cesari, ed.), pp. 47-55, Academic Press, NY, 1976.

[12] N. Wiener, The homogeneous chaos, in *Collected Works* (P. Masani, ed), pp. 572-613 (including comments by L. Gross), MIT Press, Cambridge, MA, 1976.

[13] S. Ito, S. Tanaka, and H. Nakada, On umimodal linear transformations and chaos, II, *Tokyo J. Math.* **2**, 241-259, 1979.

[14] T. Saito, On a hysteresis chaos generator, *Proceedings of the* 1985 *International Symposium on Circuits and Systems*, Vol. 2, Kyoto, pp. 847-849, 1985.

[15] Y. S. Tang, A. I. Mees, and L. O. Chua, Synchronization and chaos, *IEEE Trans. Circuits and Systems*, **30**, 620-626, 1983.

[16] R. E. Plant, The role of direct feedback in the cardiacpacemaker, in *Applied Nonlinear Analysis* (V. Lakshmikantham, ed.) pp. 309-321, Academic Press, NY, 1979.

[17] A. S. Pikovsky and M. I. Rabinovich, Stochastic oscillations in dissipative systems, *Phys. D*, **2**, 8-24, 1981.

[18] P. Stefan, A theorem of Sarkovskii on the existence of periodic orbits of continuous endomorphisms of the real line, *Comm. Math. Phys.*, **54**, 237-248, 1977.